

Effect of criticality on wetting layers: A Monte-Carlo simulation study

Nigel B. Wilding

*Department of Physics and Astronomy, The University of Edinburgh,
Edinburgh EH9 3JZ, U.K.*

Michael Krech

*Institut für Theoretische Physik, RWTH Aachen,
D-52056 Aachen, Germany*

Abstract

A solid substrate, when exposed to a vapour, can interact with it in such a way that sufficiently close to liquid-vapour coexistence a macroscopically thick liquid wetting layer is formed on the substrate surface. If such a wetting transition occurs for a binary fluid mixture in the vicinity of the critical end point of demixing transitions, critical fluctuations lead to additional long-ranged interactions (Casimir forces) within the wetting layer, changing its equilibrium thickness. We demonstrate this effect by Monte-Carlo simulations of wetting layers of a symmetrical Lennard-Jones binary fluid mixture near its critical end point. The results suggest that the effect should also be detectable in corresponding wetting experiments.

I. INTRODUCTION

Simple liquids or binary liquid mixtures in unbounded space are homogeneous and isotropic systems. In the vicinity of surfaces, however, these spatial symmetries are broken and the fluid phase diagram exhibits new surface-induced features. Principal among these are surface phase transitions such as wetting and drying which can occur when a fluid comes into contact with a solid wall [1]. These transitions are brought about by long-ranged dispersion (Van der Waals) interactions between the particles of the fluid and those comprising the wall.

Long ranged interactions of a quite different origin occur when a *critical* fluid is in contact with a wall [2,3]. Criticality is characterised by a divergent correlation length and strong order parameter fluctuations. As a result of the long range correlations, the wall modifies the properties of the critical fluid over considerable distances and this can dramatically affect surface properties such as wetting behaviour. Thus, for example, a binary liquid mixture usually demixes close to a wall due to the preferential affinity of the wall material for one of the two components [4]. If the demixing transition becomes critical, the adsorbed amount of the preferred component becomes macroscopic, a phenomenon known as critical adsorption [5,6].

If the system is constrained in more than one spatial direction, e.g. by the introduction of a second wall, the critical behaviour of the fluid is modified again. When the correlation length becomes comparable to the smallest linear extent of the system [7–9], the size dependence of thermodynamic quantities is governed by universal finite-size scaling functions. Such a finite geometry may be imposed eg. when fluids are adsorbed in slits and pores, or generated spontaneously in the course of a wetting transition eg. in a binary liquid mixture near its critical end point of demixing transitions [1,10].

An important consequence of confinement in near-critical fluids is the generation of long-ranged forces between the confining walls [11,12]. This phenomenon is a direct analogue of the well-known Casimir effect in electromagnetism [13]. Formally, the critical Casimir force arises as a result of the boundary conditions placed on the spectrum of order parameter fluctuations by the walls. This leads to a finite-size dependence for the singular part of the critical free energy, and hence a separation-dependent force between the walls [11,12]. Such critical Casimir forces are in addition to the usual dispersion forces which always exist in confined systems [14–19]. However, they differ from dispersion forces in the major respect that they are governed by *universal* scaling functions [9,11,12,20]. Precisely at the bulk critical point these scaling functions take universal values known as Casimir amplitudes [9,11,20].

Much theoretical work has been directed in recent years towards an understanding of the Casimir effect in critical systems. For the Ising universality class, (which contains the critical demixing transition of binary liquid mixtures), exact results are available in $d = 2$ dimensions for a strip geometry [21,22]. In higher dimensions, exact results are limited to the Casimir force scaling function for the spherical model [23]. For the experimentally relevant case of the $d = 3$ Ising universality class, only approximate results are available. These are based on real space renormalization [24], the field theoretic renormalization group [11,20], and Monte-Carlo (MC) simulations [20,25] for the film geometry. Other geometries have also been investigated with regard to the possibility of performing direct surface force

measurements of the Casimir force using atomic force microscopy [26,27] (see also Ref. [17]).

While the contemporary theoretical understanding of the Casimir effect in critical fluids is rather advanced, the experimental situation is not so satisfactory. Ideally, one should like to have experimental estimates of Casimir amplitudes and scaling functions to compare with theoretical estimates and to fill the gaps where no theoretical results are available. To date, however, no direct experimental demonstrations of the Casimir effect in critical fluid systems have been reported. This state of affairs seems to be attributable to the difficulties of performing high resolution surface force measurements within the extremely tight constraints of reduced temperature and pressure necessary to maintain criticality. In view of this, other more indirect routes to investigating the Casimir force have been sought. Perhaps the most promising of these is the effect of the Casimir force on wetting layers of a binary fluid mixture. If the vapour of a binary fluid is exposed to a solid substrate which strongly attracts the fluid particles, a thick liquid wetting layer will form on the substrate for state points sufficiently close to liquid-vapour coexistence. If, in addition, the temperature is chosen close to the critical end point (CEP) temperature (at which the line of critical demixing transitions intersects the liquid-vapour coexistence curve), the presence of Casimir forces within the wetting layer will change its equilibrium thickness compared to a non-critical state point of the same undersaturation [11]. Since highly accurate measurements of wetting film thicknesses are possible using modern ellipsometry techniques, this would appear a rather promising approach to probing the Casimir force experimentally. As yet, however, there have been no clear reports of such an effect in experimental wetting studies of binary fluid mixtures.

In view of the dearth of empirical results for the critical Casimir force, we have undertaken a computer simulation investigation of wetting behaviour close to the CEP of a binary fluid mixture. The aim of our study was two-fold: on the one hand to investigate the theoretical predictions of reference [11], and on the other to try to make contact with real systems by working with as realistic a simulation model as feasible. Most previous simulation work on critical phenomena in confined geometry has taken the form of MC studies of lattice gas models, favoured for reasons of their computational tractability [28,29]. Such simulations are usually performed using short-ranged surface fields to mimic the effect of walls. In this work however, we have employed an off-lattice Lennard-Jones (LJ) symmetrical binary fluid model at a planar solid wall, and have incorporated the effects of long-ranged dispersion interactions between the fluid and the wall. To our knowledge the wetting behaviour of such a system has only been previously studied for temperatures well below the consolute critical temperature [30]. Hitherto, no attempts have been made to investigate directly the effect of criticality on the formation of wetting layers either in lattice or continuum fluid models.

Our paper is organised as follows. Section II is devoted to providing some brief background material concerning the bulk phase diagram of symmetrical binary mixtures and the theory of the effect of criticality on wetting layers. In section III A we introduce our symmetrical binary fluid model and the MC simulation technique. We then detail our simulation results for the wetting behaviour of the mixture, and the influence of the critical point. Finally, in section IV we summarise and discuss our results.

II. BACKGROUND

A. Bulk phase behaviour of symmetrical binary mixtures

The simplest model for a binary fluid mixture is a symmetrical mixture in which the pure components are identical, and only the interactions between unlike particle species differ. Such a model can exhibit a variety of phase diagram topologies depending on the relative strengths of the two types of interactions. In this work, we shall be concerned with symmetrical mixtures exhibiting a critical end point. The liquid-vapour phase diagram of such a system in the density-temperature ($\rho - T$) plane is shown schematically in figure 1. At high liquid densities there exists a ‘ λ ’ line of consolute critical points. Above this line the liquid is mixed, while below the line it is demixed. As the liquid density is decreased, the demixing transition temperature moves to lower temperatures. At some point, however, the liquid phase becomes unstable with respect to the vapour. The intersection between the λ line and the liquid-gas coexistence curve marks the critical end point, which is unique as being the only point at which a critical liquid coexists with a non-critical gas.

Critical end points have been the subject of some interest in recent years on account of the singularities they induce in the first-order coexistence phase boundary (in this case the liquid-gas boundary). These singularities have been studied both theoretically [31] and by simulation [32]. One is manifest as a bulge in the liquid branch density at the CEP, as shown in figure 1. Another is found in the coexistence chemical potential. In the present work, however, we shall be concerned with the influence of the CEP on the wetting properties at the liquid-gas boundary and how it manifests the Casimir effect. In the following subsection we review existing theoretical predictions for the Casimir effect in wetting layers of a binary fluid mixture.

B. Wetting layer thickness and criticality

To analyse theoretically the wetting behaviour of the symmetrical binary fluid in the vicinity of the CEP, it is expedient to consider the phase diagram in the chemical potential-temperature ($\mu - T$) plane, as shown schematically in figure 2. Indicated on this diagram are the liquid-vapour coexistence line $\mu_{cx}(T)$, the λ line, and the CEP.

Consider now the thermodynamic path labelled \mathcal{S} in figure 2, which is given by the expression

$$\mu_{\mathcal{S}}(T) = \mu_{cx}(T) - \delta\mu, \quad (2.1)$$

where $\delta\mu > 0$ is a constant. This path runs parallel to the liquid-vapour coexistence curve and passes the critical end point on the vapour side. In the presence of a sufficiently attractive wall (complete wetting regime), and for sufficiently small undersaturations (i.e. $\delta\mu$ small), a thick liquid wetting layer will form at the wall for all points on \mathcal{S} . An expression for the thickness of such a wetting layer is obtainable by considering the layer free energy per unit area (effective interface potential) as a function of its thickness l . In the limit of an infinite wall, this is given by [11]

$$\omega(l) = l(\rho_l - \rho_v)\delta\mu + \sigma_{wl} + \sigma_{lv} + \delta\omega(l) \quad (2.2)$$

Here the first term on the right hand side represents the free energy penalty of building up a liquid layer when the vapour is the stable bulk phase. The surface tension terms σ_{wl}

and σ_{lv} contain the effects of short ranged interactions at the wall-liquid and liquid-vapour interfaces respectively, and are independent of l . The fourth term, $\delta\omega(l)$, is a finite size term incorporating both the long ranged dispersion forces and any critical finite-size effects.

Precisely at criticality, and for an infinite wall, $\delta\omega(l)$ takes the form [11]:

$$\delta\omega(l) \simeq \frac{W}{l^2} + \frac{k_B T \Delta}{l^2}. \quad (2.3)$$

In this expression, the first term on the right hand side represents the finite-size dependence of the (non retarded) dispersion forces [33], whose amplitude is given by the Hamaker constant W . The second term represents the critical finite-size contribution to the free energy [34] in three dimensions, controlled by a universal Casimir amplitude Δ , the magnitude and sign of which depend on the nature of the boundary conditions on the wetting layer. For Δ positive, the Casimir force is repulsive leading to a layer thickening, while for Δ negative, it is attractive resulting in thinning of the layer. The \simeq in eq. 2.3 indicates that we neglect any density gradient in the liquid layer that may come about because of the attractive wall potential. A density gradient implies that not all the liquid layer is precisely at criticality. However, this is expected to result in relatively small corrections to eq. 2.3.

Minimising $\omega(l)$ with respect to l yields the equilibrium layer thickness L_c at criticality:

$$L_c \simeq \left(\frac{2k_B T \Delta + 2W}{\delta\mu(\rho_l - \rho_v)} \right)^{1/3}. \quad (2.4)$$

For points on \mathcal{S} away from the CEP, however, the critical finite-size term in eq. 2.3 drops out. A useful quantity is thus the ratio of the equilibrium thickness at criticality L_c to its value L_0 away from criticality, for which one finds [12]

$$\frac{L_c}{L_0} \simeq \left(1 + k_B T_c \frac{\Delta}{W} \right)^{1/3}, \quad (2.5)$$

to leading order in $\delta\mu$. Here we have ignored any temperature dependence of the Hamaker constant.

This relationship expresses the change in thickness of a wetting layer as it becomes critical, and relates it to the Casimir amplitude Δ . As such it provides a potentially sensitive probe of the Casimir effect itself.

III. MONTE CARLO STUDIES

A. Model and simulation details

The system we have studied is a symmetrical binary fluid, having interparticle interactions of the Lennard-Jones (LJ) form:

$$u(r_{ij}) = 4\epsilon_{ij} \left[\left(\frac{\sigma_{ij}}{r_{ij}} \right)^{12} - \left(\frac{\sigma_{ij}}{r_{ij}} \right)^6 \right] \quad (3.1)$$

The following choice of parameters was made: $\sigma_{11} = \sigma_{22} = \sigma_{12} = \sigma = 1$; $\epsilon_{11} = \epsilon_{22} = \epsilon$; $\epsilon_{12} = 0.7\epsilon$. i.e. the pure components are identical, but the unlike interactions are weakened. In common with most previous simulations of LJ systems, the inter-particle potential was truncated at a distance of $R_c = 2.5\sigma$. No long-range correction or potential shift was applied.

The fluid was confined within a cuboidal simulation cell having dimensions $P_x \times P_y \times D$, in the x, y and z coordinate directions respectively, with $P_x = P_y \equiv P$. As in previous work on LJ fluids [35], the simulation cell was divided into cubic sub-cells (of size the cutoff R_c) in order to aid identification of particle interactions. Thus $P = pR_c$ and $D = dR_c$, with p and d both integers. To approximate a slit geometry, periodic boundary conditions were applied in the x and y directions, while hard walls were applied in the unique z direction at $z = 0$ and $z = D$. The hard wall at $z = 0$ was made attractive, using a potential designed to mimic the long-ranged dispersion forces between the wall and the fluid [36]:

$$V(z) = \epsilon_w \left[\frac{2}{15} \left(\frac{\sigma_w}{z} \right)^9 - \left(\frac{\sigma_w}{z} \right)^3 \right] \quad (3.2)$$

Here z measures the perpendicular distance from the wall, ϵ_w is a ‘well-depth’ controlling the interaction strength, and we set $\sigma_w = 1$. No cutoff was employed and the wall potential was made to act *equally* on both particle species.

Monte-Carlo simulations were performed using a Metropolis algorithm within the grand canonical (μ, V, T) ensemble [37,35]. Three types of Monte-Carlo moves were employed:

1. Particle displacements
2. Particle insertions and deletions
3. Particle identity swaps: $1 \rightarrow 2$ or $2 \rightarrow 1$

By virtue of the symmetry of the system, the chemical potentials μ_1 and μ_2 of the two components were set equal at all times. Thus only one free parameter, $\mu = \mu_1 = \mu_2$, couples to the density. The other variables used to explore the wetting phase diagram were the reduced well depth $\epsilon/k_B T$ and the reduced wall potential $\epsilon_w/k_B T$. During the simulations, the principal observable monitored was the total particle density profile:

$$\rho(z) = [N_1(z) + N_2(z)]/(P^2) \quad (3.3)$$

which was accumulated in the form of a histogram. Here N_1 and N_2 are the number of particles of the respective species. Other observables monitored were the total interparticle energy and the wall interaction energy.

The wetting layer thickness was obtained from the density profile as $L = \rho_l^{-1} \int \rho(z) dz$ where ρ_l is the liquid density. Although more sophisticated definitions of absolute layer thickness can be envisaged, this one is adequate for our purposes of detecting relative thickness changes arising from Casimir forces.

B. Method and results

The bulk liquid-vapour coexistence curve properties of the symmetrical LJ fluid (with $\epsilon_{12} = 0.7\epsilon$) have recently been investigated by MC simulation [32]. This work employed state-of-the-art simulation techniques to investigate the nature of coexistence curve singularities induced by the critical end point. In the course of the study, highly accurate estimates were obtained for the location of the critical end point. Additionally, the locus of the liquid-gas coexistence curve $\mu_{cx}(T)$ was measured to 5 significant figures in the neighbourhood of the CEP.

Armed with accurate estimates for $\mu_{cx}(T)$, one is in a position to perform detailed wetting studies very close to coexistence. Detailed knowledge of $\mu_{cx}(T)$ is a prerequisite for obtaining a thick wetting layer and detecting changes in its thickness due to Casimir forces. Below we discuss the procedure we have employed for detecting such changes.

Clearly for a liquid wetting layer to display critical behaviour at the bulk CEP, it must be sufficiently thick to exhibit quasi-3D properties. But for a thick wetting layer to form at a wall at all, the attractive wall potential must be sufficiently strong that complete wetting occurs at coexistence. To ensure that the CEP lay well within the complete wetting regime, a number of preliminary test runs were performed in which the temperature was set to its CEP value ($T_{cep} = 0.958$) and the density profile $\rho(z)$ monitored as coexistence was approached in a sequence of steps from the gas side. To achieve this, the chemical potential was simply increased towards its coexistence value in small increments of size $\Delta\mu = 0.0025$. The procedure was repeated for a number of different values of the wall potential ϵ_w .

For small values of $\epsilon_w/k_B T < 1.7$, it was found that the film thickness grew as coexistence was approached, but always remained finite (cf. figure 3(a)). The presence of a thin wetting layer right up to coexistence signals incomplete (partial) wetting. For stronger wall potentials ($\epsilon_w/k_B T > 1.8$), however, the film thickness became very large as coexistence was approached and ultimately almost completely filled the system (cf. figure 3(b)). This suggests that the wetting transition lies in the range $1.7 < \epsilon_w/k_B T < 1.8$. Nevertheless, to be quite sure that the CEP lay well above the wetting transition (ie. well within the complete wetting regime), all subsequent work employed $\epsilon_w/k_B T = 3.0$ at the CEP.

We have studied the layer thickness $L(\mu_S(T))$ along the path $\mu_S(T) = \mu_{cx}(T) - \delta\mu$. Given $\mu_{cx}(T)$, this path is specified solely by the value of $\delta\mu$, which has to be chosen as a compromise between two competing factors. On the one hand, $\delta\mu$ must be sufficiently small that a thick wetting layer forms. The thickness of this layer must be sufficiently large that quasi-3D critical behaviour occurs, and that the liquid-gas interfacial properties are not unduly influenced by short-ranged packing effect close to the attractive wall. On the other hand, one wishes to avoid having a layer that is very thick, lest the computational expense get out of hand. A minimum film thickness of $L = 10\sigma$ was judged sufficiently large for our purposes. However, since close to coexistence the layer thickness is extremely sensitive to changes in $\delta\mu$, fine tuning was necessary. It turned out that to obtain the required minimum thickness necessitated use of an extremely small $\delta\mu$, namely $\delta\mu = 0.002$. (corresponding to a relative undersaturation $\delta\mu/\mu \sim 10^{-3}$). At this undersaturation, L was observed to fluctuate in the range $10\sigma \lesssim L \lesssim 13\sigma$.

Another condition to be satisfied in the simulations, is that the largest fluctuation in the layer thickness be small compared to the linear extent of the system in the z direction, ie.

$L \ll D$. This latter condition ensures that the liquid gas interface does not interact with the hard-wall at $z = D$, which might otherwise obscure the effects of criticality, or even lead to capillary condensation. Accordingly the choice $D = 40\sigma$ was made.

Ideally, in order to facilitate direct contact with real systems and existing theoretical work, one should like to simulate an effectively semi-infinite system having lateral dimensions $P \gg L$. In this limit, the finite-size critical behaviour of the system depends only on the ratio ξ/L of the correlation length to the layer thickness, and not on the lateral dimensions of the simulation box [34]. Unfortunately, in this work we could not approach the semi-infinite limit as closely as we would have liked because of the huge computational expense entailed. In fact the largest lateral dimensions that we could reach were $P = 12.5\sigma$, $P = 15\sigma$ and $P = 17.5\sigma$, containing average particle numbers of approximately $N = 1500, 1800, 3500$ respectively. We postpone discussion of the effects of the relative smallness of P until later.

The limiting factor in the speed of the simulations and (hence the attainable system sizes) was found to be the extreme slowness of the interfacial fluctuations, which rendered it very difficult to accumulate accurate estimates of the average thickness. In an effort to ameliorate this problem, multi-histogram reweighting techniques were employed [38]. These allow one to combine data accumulated at individual state points and, by extrapolation, obtain estimates for observables at other not-too-distant state points. In our study the computational complexity meant that it was feasible to accumulate $\rho(z)$ at just three points on the path \mathcal{S} for each system size (see figure 2). These simulation points were chosen to span the CEP temperature, namely $T = 0.946, 0.958, 0.97$. Subsequently, the data from the individual simulations were combined self-consistently and extrapolated to yield estimates for $\rho(z)$ along the whole path. The data were collected from runs comprising in total approximately 3×10^9 Monte Carlo steps (MCS), where we define a MCS to be an attempt to perform each of the three types of MC move: particle displacement, insertion/deletion, and identity swap (cf. sec III A).

In figure 4 we present our results for the layer thickness $L(\mu_{\mathcal{S}}(T))$, obtained by implementing this procedure. The main feature of the results for each system size P , is a peak in the film thickness close to the CEP. For the largest system size, the thickness either side of the peak is fairly constant, while for the smallest system size, the accessible range of temperature was not sufficient to encompass the whole peak. For the smallest system size, the critical thickening is $\gtrsim 10\%$, while for the largest system size it is $\approx 5\%$. The peak position is at higher temperatures than the bulk CEP temperature and is closer to the CEP for the largest system size than for the smallest. The peak width also clearly narrows with increasing system size. We should caution, however, that the statistical quality of our data is not particularly high due to the difficulties mentioned above in collecting statistics. The smoothness of the temperature dependence for $L(\mu_{\mathcal{S}}(T))$ is to some extent an artifact of the histogram extrapolation procedure and we are not particularly confident of our estimates for the absolute film thickness. Nevertheless, we *are* confident of the ability of our procedure to identify *changes* in the wetting layer thickness.

The results for the film thickening due to criticality can be compared with theoretical predictions for the semi-infinite system. In this limit, the change in layer thickness is given by eq. 2.5. For our system, we calculate the Hamaker constant to be $W \approx 2.5$ at the CEP. The value of the Casimir amplitude Δ depends on the boundary conditions on the wetting layer. In the present model, these are of the form $(+, 0)$ in the notation of reference [12].

This notation denotes an order parameter (concentration) that is pinned to a constant value at the wall due to the high particle density there, and which vanishes (on average) at the liquid-gas interface because of the low gas density. The most recent field theoretical and MC estimates [20] yield $\Delta(+, 0) \approx 0.2$. Inserting this into eq. 2.5 gives $L_c/L_0 \approx 1.025$. Clearly this is a smaller thickening than we see, but the trend of our results is in the direction of this value and could lie close to the prediction for sufficiently large system size.

In fact, it is possible to use finite-size scaling arguments to account for the direction of the observed trend in peak height with increasing P . To this end, let us rewrite the finite-size part of the critical effective interface potential 2.3, taking account of the finite lateral extent of the system

$$\delta\omega(l) = \frac{W}{l^2} + \frac{k_B T_c \Delta(+, 0)}{l^2} + \frac{2l\Delta_{per}}{P^3} \quad (3.4)$$

Here we have simply added an additional scaling term to account for the finite system size P in the periodic x and y directions. The alteration to the free energy is assumed to scale like l/P , so that the contribution to $\omega(l)$ (free energy per unit area) scales like l/P^3 . This new term can be interpreted as a finite-size correction to the chemical potential.

Minimising this expression as before, gives the equilibrium critical thickness L_c . The ratio of critical to non-critical thickness then follows as

$$\frac{L_c}{L_0} = \left(1 + \frac{k_B T_c \Delta(+, 0)}{W}\right)^{1/3} \left[1 + \frac{2k_B T_c \Delta_{per}}{\delta\mu(\rho_l - \rho_v)P^3}\right]^{-1/3} \quad (3.5)$$

The Casimir amplitude for periodic boundaries has been estimated as $\Delta_{per} \approx -0.15$ [25]. Thus the correction factor in P is larger than unity and decreases towards unity as P increases. If we take the liquid-gas density difference $\rho_l - \rho_g \approx 0.5$, one finds that the correction factor is approximately 1.06 for the $P = 12.5\sigma$ system size, reducing to approximately 1.02 for the $P = 17.5\sigma$ system size. This accounts semi-quantitatively for the observed decrease in the size of the critical thickening as we increase P .

The influence of the periodic boundaries is presumably also responsible for the the observed position of the peak in $L(\mu_S(T))$. For a semi-infinite system the finite-size scaling function for $\omega(T)$ displays a peak for $T < T_{cep}$ and thus the peak in $L(\mu_S(T))$ is also expected to occur for $T < T_{cep}$. In our work, however, the peak in $L(\mu_S(T))$ occurs for $T > T_{cep}$. It seems reasonable, though, that were one to employ the finite-size scaling function for periodic boundary conditions in $\omega(T)$ then this could actually change the temperature dependence of $L(\mu_S(T))$ such that the maximum appears at some $T > T_{cep}$, if P is not much greater than L . Unfortunately, the scaling function for a system with two periodic and one symmetry breaking boundary conditions is presently not known to any approximation.

IV. CONCLUSIONS AND OUTLOOK

In summary we have performed extensive Monte-Carlo simulations of wetting behaviour near the critical end point of a symmetrical binary fluid in contact with an attractive hard wall. The results demonstrate that critical fluctuations within the wetting layer engender Casimir forces, leading to small but significant changes in the layer thickness. As such,

they constitute the first empirical evidence for the Casimir effect in a critical system. Although an unambiguous determination of the limiting size of the critical thickening was hindered by large finite-size effects, the results are in order-of-magnitude agreement with theoretical predictions for a semi-infinite system. Indeed, a theoretical analysis of finite-size corrections to this scaling limit yields estimated size effects comparable to those observed in the simulations. Given the likely magnitude of the thickening in the semi-infinite limit (which we estimate to be $\sim 3\%$), it seems likely that the effect should also be experimentally detectable in real (ie. non-symmetrical) absorbed binary fluids, many of which exhibit Hamaker constants of similar magnitude to the present model.

With regard to the computational issues raised by our study, our results testify to the capability of modern simulation techniques to identify small changes in the wetting behaviour of realistic fluid models. Indeed, simulation is likely to prove of increasing value in the study of wetting by critical layers, since unlike field theoretical or density functional methods, it allows one both to tackle realistic systems and to deal properly with critical fluctuations. Nevertheless, algorithmic improvements are clearly desirable and necessary if one is to realise geometries that are effectively semi-infinite. The chief problem experienced in this work was of extremely slow fluctuations of the liquid-gas interface. In view of this, it may well pay dividends in future work to employ a simulation algorithm that focuses more of the computational effort on the interfacial region itself, this being the bottleneck for phase space evolution. Such algorithmic improvements are the matter of ongoing work.

Finally, looking ahead to future work, it would doubtless be interesting to investigate the nature of the interfacial properties between the critical liquid and non-critical gas phases. This matter has already been the subject of a number of detailed theoretical investigations aimed at elucidating the temperature dependence of the interfacial shape and surface tension on the approach to the CEP [39,40,31]. Given present capabilities, a simulation study of interfacial properties at the CEP would certainly seem feasible and would nicely complement existing experimental studies [41,42].

ACKNOWLEDGMENTS

The authors are grateful to R. Evans for useful correspondence and to M.E. Fisher for a careful reading of the manuscript. NBW thanks K. Binder and V. Privman for helpful discussions, and the Royal Society of Edinburgh for financial support. MK gratefully acknowledges financial support through the Heisenberg program of the Deutsche Forschungsgemeinschaft.

REFERENCES

- [1] S. Dietrich in *Phase Transitions and Critical Phenomena*, edited by C. Domb and J.L. Lebowitz (Academic, London, 1988), Vol.12, p. 1.
- [2] K. Binder in *Phase Transitions and Critical Phenomena*, edited by C. Domb and J.L. Lebowitz (Academic, London, 1983), Vol.8, p. 2.
- [3] H.W. Diehl in *Phase Transitions and Critical Phenomena*, edited by C. Domb and J.L. Lebowitz (Academic, London, 1986), Vol.10, p. 76.
- [4] M.E. Fisher and H. Au-Yang, *Physica A* **101**, 255 (1980).
- [5] H.W. Diehl and A. Ciach, *Phys. Rev. B* **44**, 6642 (1991).
- [6] H.W. Diehl and M. Smock, *Phys. Rev. B* **47**, 5841 (1993).
- [7] M.E. Fisher, in *Proceedings of the 1970 Enrico Fermi School of Physics, Varenna, Italy*, Course No. LI, edited by M.S. Green (Academic, New York, 1971), p. 1; M. E. Fisher and M.N. Barber, *Phys. Rev. Lett.* **28**, 1516 (1972).
- [8] M.E. Fisher and H. Nakanishi, *J. Chem. Phys.* **75**, 5857 (1981).
- [9] M.N. Barber, in *Phase Transitions and Critical Phenomena*, edited by C. Domb and J.L. Lebowitz (Academic, New York, 1983), Vol. 8, p. 145; V. Privman, in *Finite Size Scaling and Numerical Simulation of Statistical Systems*, edited by V. Privman (World Scientific, Singapore, 1990).
- [10] M.P. Nightingale and J.O. Indekeu, *Phys. Rev. Lett.* **54**, 1824 (1985) and *Phys. Rev. Lett.* **55**, 1700 (1985); R. Lipowski and U. Seifert, *Phys. Rev. B* **31**, 4701 (1985) and *Phys. Rev. Lett.* **55**, 1699 (1985).
- [11] M. Krech and S. Dietrich, *Phys. Rev. A* **46**, 1886 (1992).
- [12] M. Krech, *The Casimir Effect in Critical Systems* (World Scientific, Singapore, 1994) and references therein.
- [13] L. Spruch, *Science* **272**, 1452 (1996) and references therein.
- [14] S.L. Carnie, D.Y.C. Chan, and J. Stankovich, *J. Coll. Int. Sci.* **169**, 116 (1994).
- [15] G.H. Nyland and I. Brevik, *Physica A* **202**, 81 (1994); I. Brevik and G.H. Nyland, *Ann. Phys.* **230**, 321 (1994).
- [16] S. Leseduarte and A. Romeo, *Ann. Phys.* **250**, 448 (1996).
- [17] P. Johansson and P. Apell, *Phys. Rev. B* **56** 4159 (1997).
- [18] M.Y. Novikov, A.S. Sorin, and V.Y. Chernyak, *Theor. Math. Phys.* **91**, 658 (1992) and **92**, 773 (1993).
- [19] M. Borday, G.L. Klimchitskaya, and V.M. Mostepanenko, *Phys. Lett. A* **200**, 95 (1995).
- [20] M. Krech, *Phys. Rev. E* **56** 1642 (1997).
- [21] J.L. Cardy, *Nucl. Phys. B* **275**, 200 (1986).
- [22] R. Evans and J. Stecki, *Phys. Rev. B* **49**, 8842 (1994).
- [23] D. Danchev, *Phys. Rev. E* **53**, 2104 (1996).
- [24] J.O. Indekeu, M.P. Nightingale, and W.V. Wang, *Phys. Rev. B* **34**, 330 (1986).
- [25] M. Krech and D.P. Landau, *Phys. Rev. E* **53**, 4414 (1996).
- [26] T.W. Burkhardt and E. Eisenriegler, *Phys. Rev. Lett.* **74**, 3189 (1995); E. Eisenriegler and U. Ritschel, *Phys. Rev. B* **51**, 13717 (1995).
- [27] S. Gnutzmann and U. Ritschel, *Z. Phys. B* **96**, 391 (1995).
- [28] K. Binder and D.P. Landau, *Physica A* **177**, 483 (1991).
- [29] K. Binder and D.P. Landau, *J. Chem. Phys.* **96**, 1444 (1992).
- [30] Y. Fan, J.E. Finn and P.A. Monson, *J. Chem. Phys.* **99**, 8238 (1993).

- [31] M.E. Fisher and P.J. Upton, Phys. Rev. Lett. **65**, 3405 (1990). M.C. Barbosa and M.E. Fisher, Phys. Rev. **B43**, 10635 (1991); M.C. Barbosa, Phys. Rev. **B45**, 5199 (1992).
- [32] N.B. Wilding, Phys. Rev. Lett **78**, 1488 (1997); N.B. Wilding, Phys. Rev. **E55**, 6624 (1997).
- [33] P.G. de Gennes, J. Phys. Lett (Paris) **42**, L377 (1981).
- [34] M.E. Fisher and P.G. de Gennes, C.R. Acad. Sc. Paris, **287**, 207 (1978).
- [35] N.B. Wilding, Phys. Rev. **E52**, 602 (1995).
- [36] J. Israelachvili *Intermolecular and surface forces* (Academic Press, London, 1992).
- [37] M.P. Allen and D.J. Tildesley *Computer simulation of liquids* (Oxford University Press, London, 1987).
- [38] A.M. Ferrenberg and R.H. Swendsen, Phys. Rev. Lett. **61**, 2635 (1988); *ibid* **63**, 1195 (1989).
- [39] B. Widom, J. Chem. Phys. **67**, 872 (1977).
- [40] M.M. Telo da Gama, R. Evans, Mol. Phys. **48**, 229 (1983); *ibid* **48**, 251 (1983); M.M. Telo da Gama, R. Evans and I. Hadjiagapiou, Mol. Phys. **52**, 573 (1984);
- [41] B.M. Law, Phys. Rev. Lett. **67**, 1555 (1991).
- [42] D.S.P. Smith and B.M. Law, J. Chem. Phys. **99**, 9836 (1993).

FIGURES

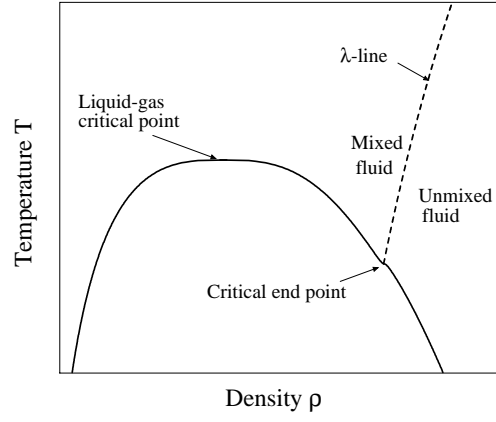


FIG. 1. Schematic representation of the phase diagram of a symmetrical binary fluid mixture in the density-temperature plane. The full curve is the liquid-gas coexistence envelope. The dashed curve is the λ -line of critical demixing transitions. The two curves intersect at the critical end point. The singularity in the liquid branch at the CEP is also shown [32].

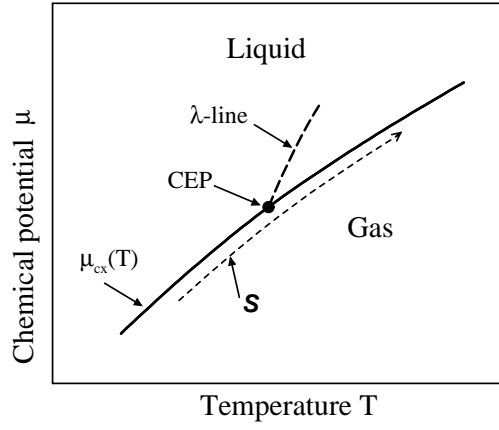


FIG. 2. Schematic phase diagram of a symmetrical binary fluid. The full curve is the first order liquid-gas phase coexistence line $\mu_{cx}(T)$. The dashed curve is the critical (λ) line of second order transitions separating the mixed and demixed liquid phases. The two curves intersect at the critical end point. Also shown is a path S parallel to $\mu_{cx}(T)$ on the gas side.

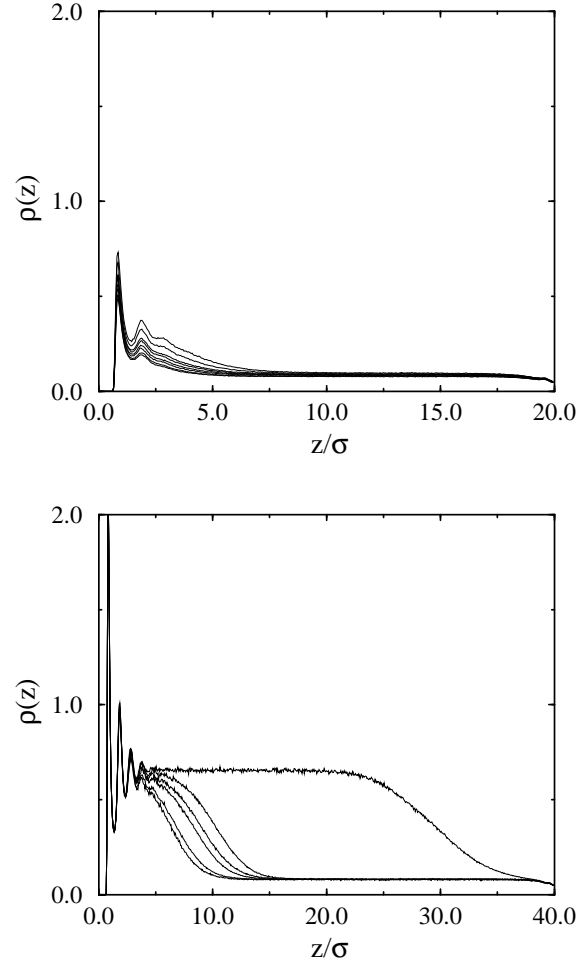


FIG. 3. **(a)** Density profiles $\rho(z)$ on the approach to coexistence for $\epsilon_w = 1.7$. The film thickness remains small right up to coexistence signifying incomplete wetting. **(b)** Density profiles for $\epsilon_w = 1.8$. The film thickness grows very large as coexistence is approached, signifying complete wetting.

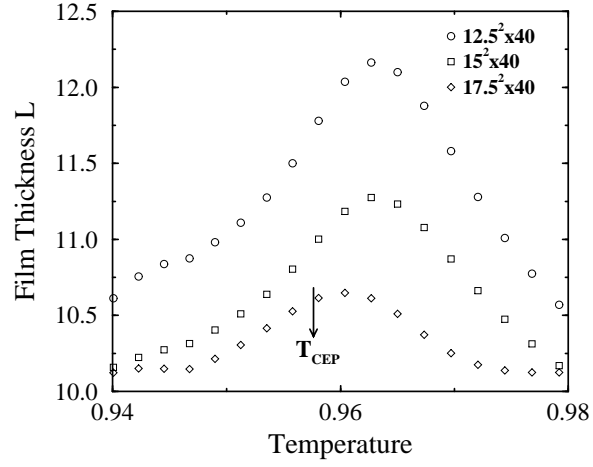


FIG. 4. The thickness of the wetting layer as a function of temperature along the thermodynamic path \mathcal{S} defined in the text. Data is shown for each of the three system sizes studied. The results were obtained from multihistogram extrapolation of simulation data accumulated at three points on this line, corresponding to temperatures $T = 0.946, 0.958, 0.97$.